Available online at www.sciencedirect.com
ScienceDirect
Journal of Marine Systems 68 (2007) 318–326
JOURNAL OF MARINE SYSTEMS
www.elsevier.com/locate/jmarsys

Tropical cyclone genesis over the south China sea

Guihua Wang [a,*], Jilan Su [a], Yihui Ding [b], Dake Chen [a,c]

[a] State Key Laboratory of Satellite Ocean Environment Dynamics, Second Institute of Oceanography, State Oceanic Administration, Hangzhou, China
[b] National Climate Center, China Meteorological Administration, Beijing, China
[c] Lamont-Doherty Earth Observatory of Columbia University, New York, USA

Received 29 June 2005; received in revised form 10 October 2006; accepted 11 December 2006
Available online 22 December 2006

Abstract

The South China Sea (SCS) is among areas in the Northwest Pacific most frequented by tropical cyclones (TCs) with intensity reaching a tropical storm or stronger. It is also an area of significant TC genesis. In this study, TC genesis in SCS and its monsoonal variability for 1948–2003 are analyzed. Altogether, in May–September (southwest monsoon period) 157 TC geneses have occurred north of 12°N in SCS, while in October–December (northeast monsoon period) 64 out of 65 TC geneses have happened south of 18°N. It is found that the monsoonal characteristics of the SCS basically determine the region of TC genesis in each monsoon season. Winter TC genesis in the SCS happens over the region where the marine environment satisfies the four criterions on, respectively, the sea surface temperature (SST), mid-troposphere relative humidity, vertical shear of the horizontal winds and low-level atmospheric vorticity. During the summer, as the two criterions on SST and the mid-troposphere relative humidity are satisfied for the whole SCS, TC genesis occurs in the region where both the low-level vorticity and the vertical shear satisfy the criterion. In addition, there is likely more TC genesis in the winter during the onset of La Nina, and more TC genesis in the summer following the onset of El Nino.
© 2006 Elsevier B.V. All rights reserved.

Keywords: Tropical cyclones; Genesis; Monsoon; Air–sea interaction; South China Sea

1. Introduction

The South China Sea (SCS), the largest semi-enclosed marginal sea in the Northwest Pacific with an area about 3.5×10^6 km^2 (Fig. 1), is under the influence of the East Asia Monsoon (Liang, 1991). Onset of the mild southwesterly summer winds over the SCS usually occurs suddenly around mid-May in its southern and central part and soon expands to the entire SCS in June. In contrast, the strong northeast winter monsoon is established progressively over the SCS, first appearing over its northern part in September, reaching its central in October and covering the entire SCS in November. The winter monsoon gradually diminishes in April. Most of the oceanic characteristics of the SCS are influenced by the monsoon.

As in many research works, here we define the tropical cyclone (TC) as a tropical mesoscale cyclonic weather system with its strength of a tropical storm or stronger (i.e., typhoon). Globally, the Northwest Pacific, including the SCS, has the most TCs. Based on data spanning over 1968–1988 (Neumann, 1993), the annual average numbers of TC and typhoon generated in the

* Corresponding author.
E-mail address: guihua_wanggh@yahoo.com.cn (G. Wang).

0924-7963/$ - see front matter © 2006 Elsevier B.V. All rights reserved.
doi:10.1016/j.jmarsys.2006.12.002

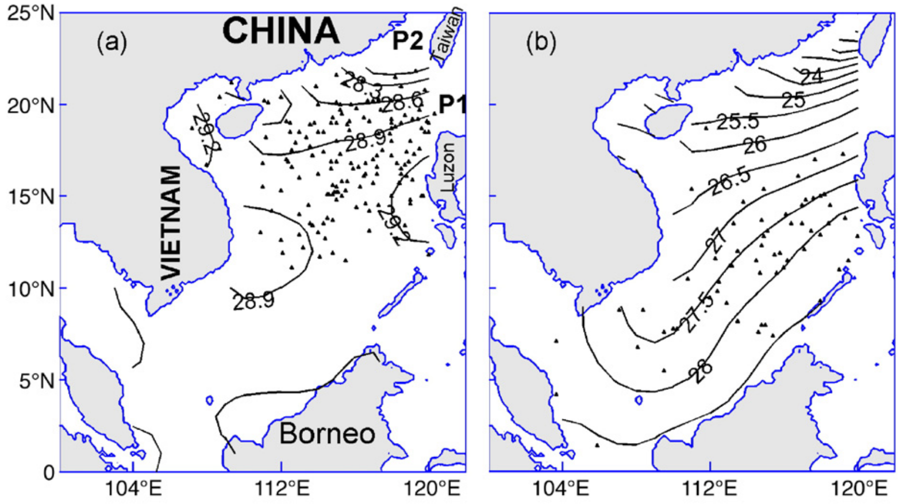

Fig. 1. SST climatology (in °C) and the initial positions of TCs (solid triangle) over the SCS for 1948–2003 (P1: Luzon Strait; P2: Taiwan Strait.). a: Southwest monsoon period; b: northeast monsoon period.

Northwest Pacific are 25.7 and 16.0, respectively. SCS is among the areas in the Northwest Pacific most often frequented by TCs. In addition, SCS itself is also an area of significant TC genesis. Our TC dataset shows that, among the annual average of 10.3 TCs passing through the SCS, 3.5 originated within the SCS. For typhoons, the corresponding numbers are 6.0 and 1.3, respectively.

TC is a tropical mesoscale weather system operating on the feedback between the enthalpy fluxes and winds at the ocean surface (Emanuel, 2003). It may be regarded as a heat engine with heat-intake over the ocean, a nearly adiabatic work-output in the eyewall and heat-loss near the stratosphere (Lighthill, 1998). In this system, TC genesis depends critically on the conditions at the air–sea surface and on the surrounding atmospheric environment. As summarized by Emanuel (2003), there are 6 necessary, or conducive, oceanic and atmospheric environmental conditions for TC genesis, namely,

(1) High sea surface temperature (SST): an ocean with SST at least 26 °C to provide sufficient latent-heat input to fuel the winds of a TC (Lighthill, 1998). However, Chen (1981) has found that an SST above 27 °C is a pre-requisite for TC genesis over the SCS. This will be the value we shall adopt for this study;
(2) Sufficiently large depths of the ocean mixed layer;
(3) An atmospheric environment characterized by large values of mid-troposphere relative humidity: necessary for sustained development of a TC. Otherwise, the extremely dense cloud eyewall of the TC will be dried out by upflow of the entrained dry ambient air (Lighthill, 1998). If the relative humidity at 500 mb (RH) is lower than 40%, formation of TCs will be inhibited (Gray, 1968);
(4) Small vertical shear of the horizontal winds: important for the TC development for allowing the heat released by condensation to concentrate in a vertical column (Fink and Speth, 1998). Gray (1968) proposed to characterize the vertical shear with $|V_z|$, the magnitude of the horizontal wind difference between the upper and lower troposphere, i.e., 200 mb and 850 mb, respectively. Local $|V_z|$ greater than 8 ms^{-1} is generally unfavorable for TC development (e.g., Goldenberg et al., 2001);
(5) An atmospheric background with relatively large cyclonic low-level vorticity: producing initially a frictionally forced low-level convergence of mass and water vapor, and consequently leading to an upward vertical motion in favor of TC genesis (Gray, 1968); and
(6) A non-negligible Coriolis force, usually at latitudes beyond 5° from the equator, to maintain the cyclonic circulation.

The first 3 are thermodynamic conditions, while the last 3 are dynamical ones. In addition, an external disturbance is also needed to trigger the TC genesis.

Previous studies have shown that TC genesis over the SCS happens predominantly at its northern basin in summer (Liang, 1991), while in winter it favors the southern SCS (Liang et al., 1998). Liang (1991) suggested that many external disturbances from atmosphere circulation over the SCS are responsible for the TC genesis.

The lifespan of these TCs is relatively short, lasting only 3–4 days. Statistical parameters of their life history are listed in Table 1. Though previous studies presented the possible linkage between TCs and large scale tropical circulation (for example, Chu, 2004; Harr and Chan, 2005), how the ocean and monsoon environments affect SCS TCs have not been explored in detail.

In this paper, detailed analysis of the seasonal and interannual environmental conditions of the SCS for TC genesis is carried out, with special attention to their connection with the monsoon characteristics. External disturbances for the development of the TCs are also addressed briefly.

2. Data

Our TC dataset covers the period of 1948–2003. The year 1948 is chosen because it is the starting year of the National Centers for Environmental Prediction (NCEP) wind data. The TC data are derived from two TC datasets, one provided by the National Oceanic and Atmospheric Administration (NOAA) of USA and the other the Japan Meteorological Agency (JMA). The former dataset spans 1945–1998 and the latter 1953–2003. For the period of 1948–1952 or 1999–2003, only the NCEP or JMA product, respectively, is used. The two products are merged for the period 1953–1998 because of the difference in these two datasets. The JMA data covers only TCs as defined in this study, while the NOAA data includes, in addition to TCs, also some but not all tropical mesoscale cyclonic weather systems with strength weaker than the tropical storm. We therefore concentrate only on TCs for this study. The two datasets show identical TCs since 1992 but have close to 14% discrepancy in TC identity before 1992. This may be due to different data sources or different methods of analysis used to construct the two datasets. Data in both files include 6-hourly positions of each TC, as well as its associated minimum center pressure and maximum wind speed. We choose from both datasets all the TCs that have occurred over the SCS, defined for this purpose as the area (0–22.5°N, 98.5–120.5°E), in 1948–2003.

The wind and relative humidity product are from the NCEP data, available from 1948 to present. They have a one-month temporal resolution and a 1.875° Gaussian grid spatial resolution. The SST data are from Had1SST, a dataset provided by the Hadley Center of the UK Met Office, which has a one-month temporal resolution and a $1° \times 1°$ spatial resolution (Rayner et al., 2003).

To study the growth of TCs from initial tropical disturbances, we use the cloud satellite images from the Stretched Visible and Infrared Spin Scan Radiometer (S-VISSR) Data provided by the Institute of Industrial Science, University of Tokyo. The available S-VISSR data is from 1997 to 2003 with an hourly time resolution. Tropical disturbances are defined as a distinctly organized cloud pattern of a spatial scale of 100 to 300 km, with a corresponding wind pattern in the range of 100 to 600 km. As both Gray (1968) and Liang (1991) have demonstrated, the tropical disturbances can be traced well from satellite pictures and wind fields.

3. Seasonal variation of the TC genesis

Altogether 222 TCs are identified to have been generated in the SCS during the 56 years of 1948–2003.

Table 1
Statistics of the life history of TCs generated over the SCS

Month	Number	Distance (km)			Life time (days)			Speed (km/day)			Strength (m/s)		
		Max	Min	Mean	Max	Min	Mean	Max	Min	Mean	Max	Min	Mean
Jan	0	0.00	0.00	0.00	0.00	0.00	0.00	0.00	0.00	0.00	0	0	0
Feb	1	8.60	8.60	8.60	3.00	3.00	3.00	2.87	2.87	2.87	45	45	45
Mar	0	0.00	0.00	0.00	0.00	0.00	0.00	0.00	0.00	0.00	0	0	0
Apr	4	9.00	2.73	5.65	5.75	1.00	3.00	2.86	1.57	2.10	55	25	40
May	17	91.78	8.29	29.53	12.25	4.25	7.51	8.92	0.94	3.74	85	30	53
Jun	24	74.64	3.55	16.89	11.75	1.25	5.19	6.35	0.73	3.00	120	30	51
Jul	26	31.12	3.71	11.39	9.25	1.25	4.83	4.37	0.82	2.51	90	30	53
Aug	48	79.19	0.60	12.83	21.25	0.50	5.17	14.88	0.27	3.30	90	30	51
Sep	41	45.12	2.25	11.24	15.75	0.75	5.21	5.90	0.44	2.56	130	25	60
Oct	26	73.66	5.54	13.29	17.50	1.75	5.06	7.96	0.58	2.99	100	25	53
Nov	22	31.67	1.04	10.19	9.50	0.50	3.93	10.61	1.03	3.02	140	35	56
Dec	13	16.72	1.49	7.41	8.50	2.00	4.15	3.45	0.17	2.15	75	30	41
Summer	157	64.37	3.68	16.38	14.05	1.60	5.58	8.08	0.64	3.02	103	29	53.6
Winter	60	40.68	2.69	10.30	11.83	1.42	4.38	7.34	0.59	2.72	105	30	50.0

Distance is the straight line between the initial and end positions of a TC. Summer (winter) denote the southwest (northeast) monsoon period.

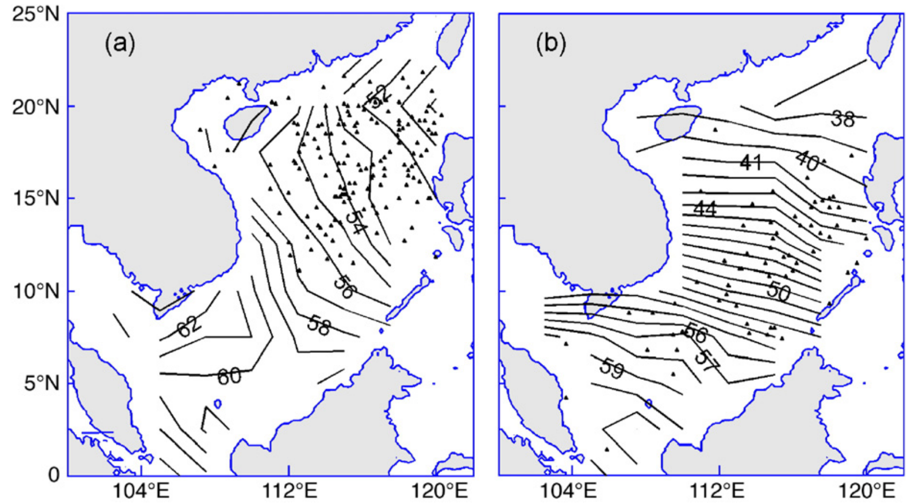

Fig. 2. RH climatology (in %) and the initial positions of TCs (solid triangle) over the SCS for 1948–2003. a: Southwest monsoon period; b: northeast monsoon period.

Most of these TCs have originated in May to December, ranging from a maximum of 48 in August and a minimum of 13 in December. TC genesis is rather rare in late winter monsoon (January to April), with no TC generated in either January or March, only 1 in February and 4 in April. In the following analysis we shall exclude the late winter monsoon period from our climatology study. However, we shall discuss briefly the environmental conditions underlying the 5 TCs generated during the late winter monsoon period. For convenience of classification we define, for this study, the 5 months from May to September as the southwest monsoon period and the 3 months from October to December the northeast monsoon period. Altogether there are 157 (65) TCs generated during the southwest monsoon period (northeast monsoon period). The initial positions of the TCs formed in the southwest monsoon period are above 11°N, while, except for 3 TCs, those formed in the northeast monsoon period tend to be on the south side between 5°N and 18°N (Fig. 1). Since the oceanic and atmospheric conditions are vastly different between the two monsoon periods, we present the summer and winter environments separately.

3.1. Southwest monsoon period

Fig. 1a shows the SST climatology of the SCS for the southwest monsoon period. The climatological summer mean SST is greater than 28.5 °C everywhere except very near the Taiwan Strait. Over most of the SCS outside the Chinese coast, SST is actually higher in June than in August. This is due to a combination of the spreading of the cold filament from coastal upwelling near Vietnam, reflected as the cold center off central Vietnam in Fig. 1a, after the onset of southwest monsoon and the open-ocean upwelling driven by a strong southwest wind jet (Xie et al., 2003). This wind jet is a result of the orographic effect of an over 500 m mountain range in central Vietnam on the prevailing southwesterly winds.

The climatological summer mean RH is greater than 40% over the whole SCS (Fig. 2a). This is consistent with the understanding that, during the southwest monsoon period, moisture originated from the Southern Hemisphere and the Indian Ocean forms a continuous channel flowing into the Asian region, supplying ample moisture to SCS (Ding et al., 2004).

The climatological summer mean $|V_z|$ is less than 8 ms^{-1}, required for TC genesis, over the SCS areas only to the north of about 8°N (Fig. 3a). This distribution agrees with the findings of Wang and Fan (1999) that southwest monsoon over SCS is characterized by intensified easterlies at 200 mb across a broad region below about 10°N and by enhanced westerlies at 850 mb in a narrow latitude belt between 5°N and 15°N.

The climatological summer mean zero low-level vorticity line runs from the Gulf of Thailand to the west coast of north Luzon (Fig. 4a). This line follows generally the core of the persistent strong southwest wind jet in summer, as mentioned above. The climatological summer mean vorticity is positive north of this line and negative south of it. It is known that, subsequent to the summer monsoon onset the 850 mb winds over the

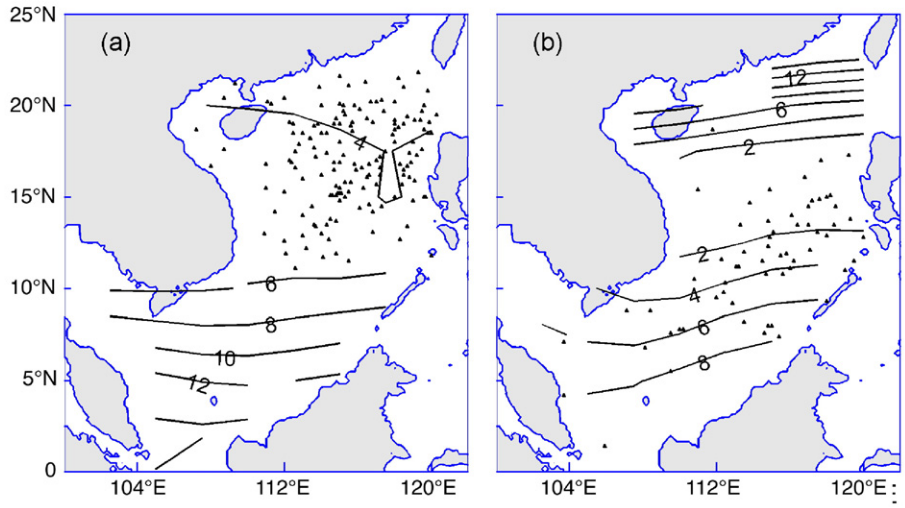

Fig. 3. $|V_z|$ climatology (in ms^{-1}), and the initial positions of TCs (solid triangle) over the SCS for 1948–2003. a: Southwest monsoon period; b: northeast monsoon period.

northern SCS experiences a quick switch from anticyclonic to cyclonic (e.g., Wang and Wu, 1997).

Table 2 summarizes, in a general sense, the regions of the SCS where climatology monsoonal mean environment satisfies, respectively, the TC genesis criterion for Conditions (1), (3), (4) and (5) on, respectively, SST, RH, $|V_z|$ and low-level vorticity. Quantified criterions for Condition (1), (3) and (4) have been given above. For Condition (5), however, no such reference has been found and we simply take positive value as its criterion for our discussion. During the southwest monsoon period over 1948–2003, TC geneses in SCS have occurred largely in the region north of 10°N. As both the SST and RH criterions are satisfied over the whole SCS, distributions of the vorticity and vertical shear are likely to be critical in deciding that the TC genesis takes place in the northern, rather than the southern, SCS during the southwest monsoon.

As commented previously, an external disturbance is needed to trigger the TC genesis. Disturbances from mesoscale systems in the SCS such as frontal systems in the northern SCS, for example, have evolved into TCs (Wang and He, 1979). Fig. 5a shows the initial position

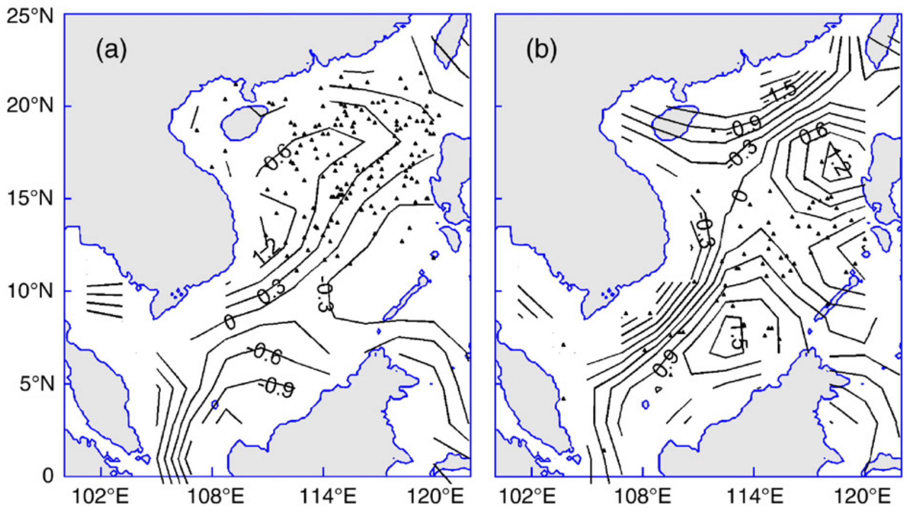

Fig. 4. ζ climatology (in 10^{-5} s^{-1}), solid lines positive and dashed lines negative, and the initial positions of TCs (solid triangle) over the SCS for 1948–2003. a: Southwest monsoon period; b: northeast monsoon period.

Table 2
Regions in SCS where all four climatological monsoonal means (SST, RH, $|V_z|$ and ζ) satisfy the corresponding TC genesis criterions

Season	SST	RH	$\|V_z\|$	ζ
Southwest monsoon	All SCS	All SCS	N of 8°N	NW
Northeast monsoon	SE half	S of 11°N	5–18°N	SE 3/4th

N: north; S: south; NW: northwest; SE: southeast.

of 29 disturbances during the southwest monsoon period in 1997–2003, which have developed into TCs first appearing in the SCS. Among these 29 cases, only 1 (3%) has originated from the Western Pacific outside of the SCS. The other 28 disturbances seem to have originated within the SCS itself. The initial positions of 14 of these 28 disturbances are at the windward area of the mountain ranges on both the Luzon and Taiwan Islands with orographically induced strong mesoscale convective systems (Xie et al., 2006), which can serve as the initial disturbances for the TCs. Of these 14 TCs northwest or west of Luzon, 9 of them can also be identified as having evolved from the moist monsoon trough, where convective disturbances are often found (Chu, 2004). The summer monsoon trough usually runs across the northern SCS (Tao and Chen, 1987). Evolution of the remaining 14 disturbances is difficult to follow from our dataset. Those at the northern SCS are likely triggered from instabilities of the frontal system observed previously by Wang and He (1979) or from the easterly waves as described by Liang (1991).

3.2. Northeast monsoon period

During the northeast monsoon period, the climatological SST isotherms over 27 °C have a northeast–southwest orientation and the 27 °C isotherm itself runs from the northern Luzon coast to the central Vietnam coast (Fig. 1b). This feature is due to advection of the cold water from the northern SCS by the southward western boundary current (Liu et al., 2004; Su, 2004).

Distribution of the RH climatology over SCS for the northeast monsoon period (Fig. 2) can be understood with the so-called East Asian local Hadley cell structure (Chang et al., 1979). The lower troposphere northeasterly winds, reinforced intermittently by cold dry air surges from the Siberian High, ascend with strong convection over the equatorial trough. As a result, deep cumulus layer develops over the central and southern SCS (Johnson and Zimmerman, 1986). Thus, during this period the RH over the SCS is greater than 40% only south of about 17°N (Fig. 2b). In fact, it is further south next to Luzon because this area is the dry leeward side of the northeast winds with much enhanced strength from the orographical effects of the high mountain ranges over Luzon (Wang et al., submitted for publication).

Associated with the local Hadley cell discussed above there is a 200 mb East Asian westerly jet stream in winter (Zhang et al., 1997). The jet lies north of about 15°N over the SCS and is associated with intense baroclinicity and large vertical wind shear. This is reflected in the $|V_z|$ climatology (Fig. 3b) where we find $|V_z|$ larger than 8 ms^{-1} north of around 20°N in SCS, unfavorable for TC development. The vertical shear is lower than 8 ms^{-1} between 6–15°N, favorable for TC genesis.

Fig. 4b shows the low-level vorticity climatology over the SCS for the northeast monsoon period. Combined effects of the Siberia High and Equatorial Trough during the northeast monsoon result in the prevailing low-level northeast winds over the SCS, confined mainly below 700 mb (Chang et al., 1979). The axis of the wind maximum, i. e., the zero low-level vorticity line, runs from northeast–southwest across the central SCS, with

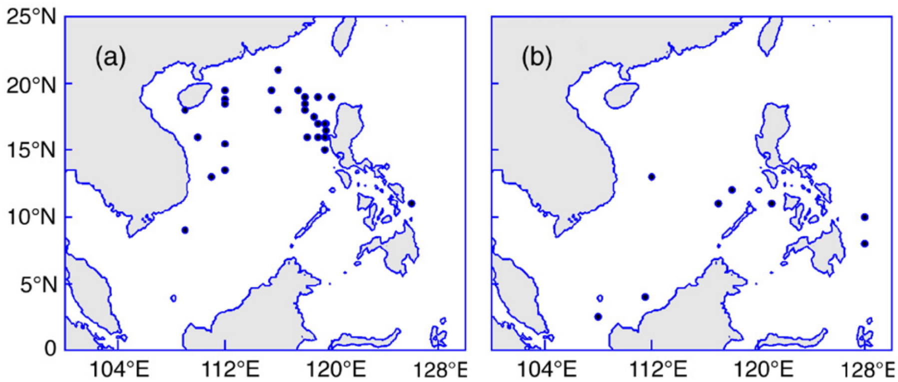

Fig. 5. Initial position of disturbances developed into TCs first appearing in the SCS during 1997–2003. a: Southwest monsoon period; b: northeast monsoon period.

anticyclonic wind shear over the northwest SCS and cyclonic over the southeast (Chen and Ding, 1979; Ding, 1994). The distribution in Fig. 4b basically reflects such a pattern. High positive vorticity values west of Luzon are the result from orographic effects of the prevailing northeasterly monsoon winds (Wang et al., submitted for publication).

Generally, we see that the criterions of SST, RH, $|V_z|$ and relative vorticity for TC genesis are satisfied over the southeastern half of the SCS during the northeast monsoon period (Table 2).

Fig. 5b shows the initial position of 8 disturbances for the northeast monsoon period of 1997–2003, which have developed into TCs first appearing in the SCS. 3 of the 8 disturbances (37.5%) have originated from the Western Pacific or Sulu Sea and then have moved into the SCS. 6 of the 8 disturbances (75%) are associated with the Inter-Tropical Convergence Zone (ITCZ), based on the S-VISSR images. Similar conclusion has also been reached early by Liang (1998), using GMS VISSR images from 1985–1994.

4. Interannual variation of the TC genesis

Interannual variability of the tropical cyclone activity in the SCS has been related to ENSO (Liang et al., 1998). Here we provide some evidences to demonstrate possible ENSO impacts on the annual number of TC genesis in the

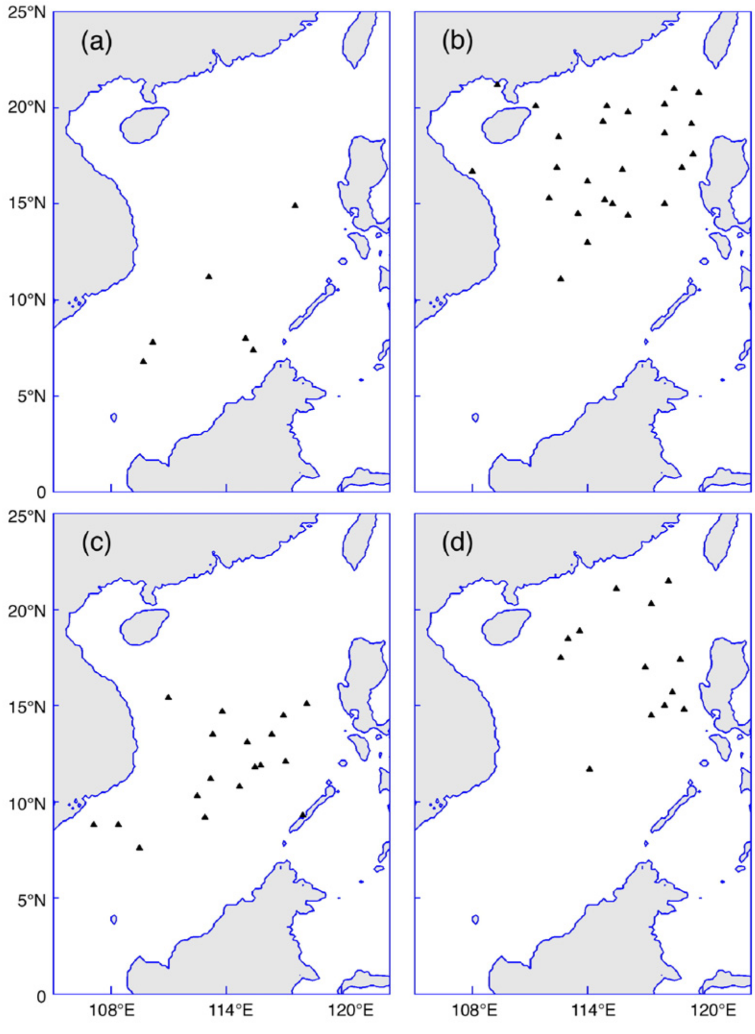

Fig. 6. Initial positions of the tropical cyclones during El Nino Years (1957, 1965, 1972, 1982, 1991 and 1997) and La Nina Years (1955, 1970, 1973, 1975, 1988 and 1998). a: Northeast monsoon period in El Nino Years; b: southwest monsoon period in El Nino Years; c: northeast monsoon period in La Nina Years; d. southwest monsoon period in La Nina Years.

Table 3
Number of TCs with genesis occurred where the climatological monsoonal mean environment does not meet one of the TC genesis criterions (1), (3), (4) and (5), respectively

Season	SST	RH	$\lvert V_z \rvert$	ζ
Southwest monsoon	None	None	None	17
Northeast monsoon	1	3	1	4

SCS. Initial positions of TCs for the six strong warm events of 1957–58, 1965–66, 1972–73, 1982–83, 1991–92 and 1997–98 and six strong cold events of 1955–56, 1970–71, 1973–74, 1975–76, 1988–89 and 1998–99 are shown in Fig. 6. In this figure, SWMP denotes the summer period in the year following the onset of El Nino or La Nina. The average yearly numbers of TC genesis in the SCS for 1948–2003, the 6 warm events and the 6 cold events are, respectively, 1.1, 1.0 and 2.8 for the northeast monsoon period, and 2.8, 4.0 and 2.2 for the southwest monsoon period. Thus, in the SCS, there is likely more TC genesis in the winter during the onset of La Nina, and more TC genesis in the summer following the onset of El Nino. We now return to the 5 TCs generated during the late winter (from January to April) monsoon in 1948–2003, 1 in February and 4 in April. Of the 5 TCs, 4 were also generated during cold episodes (La Nina) of ENSO (1956, 1965, 1996 and 1999) and 1 in a neutral year, 1961.

An examination of the TC-genesis Conditions (1), (3), (4) and (5) indicates that significantly increased cyclonic low-level vorticity during the northeast monsoon period of a cold event may be the cause for its enhanced TC genesis. As for the enhanced TC genesis during the southwest monsoon period of a warm event, conditions of SST and RH for the region occupied by the overall initial positions of TCs (Fig. 1) all become more favorable for TC genesis, whereas both $\lvert V_z \rvert$ and low-level vorticity have become slightly unfavorable but still satisfy the criterion. Considering the average conditions of the SCS the southwest monsoon period of 1948–2003 (Figs. 1–4), the increase of 0.4 °C for SST over the northern SCS seems to be the principal contributing factor to the increasing TC genesis.

As to the disturbances triggering the TC genesis, increased convective activity during the northeast monsoon period of a cold event (Chu, 2004) may be another cause for its enhanced TC genesis. For the southwest monsoon period, Chang et al. (2000) has shown that the moist monsoon trough is significantly intensified during a warm event. This may result in, as commented above, more mesoscale convective systems, providing more triggering disturbances for TC genesis.

5. Summary and discussion

Using several datasets, we have examined the environments of the SCS for Conditions (1), (3), (4) and (5) for TC genesis. It is found that, overall speaking, fulfillment of these four conditions correlates well with the seasonal (monsoonal) characteristics of the TC genesis. Interpretation for its interannual characteristics is also consistent with these four conditions. It would be worthwhile to examine how the distribution of the ocean mixed layer depths, i.e., Condition (2), is related to the TC genesis. However, our datasets do not provide such information for our study. As to the latitudinal dependence of the TC genesis, i.e., Condition (6), only two winter TC genesis have occurred below 5°N (Fig. 1). Chang et al. (2003) have discussed the conditions in December 2001 leading to the genesis of the southern most one near 1.5°N.

Out of the 157 (65) TCs generated in May–September, the southwest monsoon period (October–December, northeast monsoon period), over 10% happened in areas where the 1948–2003 climatology monsoonal mean environment do not entirely meet all the four criterions (Table 3). When the monthly mean environmental data are used, the percentage is reduced to around 5% for both periods (Table 4). In this case, only 8 summer (4 winter) TC geneses have occurred under below-criterion value in vorticity and another 1 winter TC genesis under below-criterion value in the relative humidity. Since the NCEP wind dataset is a highly smoothed one, improved wind data such as QuikSCAT may further reduce the cases with below-criterion value in vorticity. In addition, because of the short lifespan of TCs formed in SCS and of the intermittent nature of the winds, weekly mean environment data may also improve on the uncertainty.

Disturbances developing into TCs in the SCS arise from many possible atmospheric systems. The identified time period for a disturbance to develop into a TC is about 5–28 h, with an average period of 12 h. The identified travel distance of a disturbance from its birth to the TC state is about 15–500 Km, with an average distance of 300 Km. In this study we have not analyzed how these disturbances have developed into TCs.

Table 4
Number of TCs with genesis occurred where the climatological monthly mean environment does not meet one of the TC genesis criterions (1), (3), (4) and (5), respectively

Season	SST	RH	$\lvert V_z \rvert$	ζ
Southwest monsoon	None	None	None	8
Northeast monsoon	None	1	None	4

Acknowledgements

This study was supported by the NSFC Grant (G40676007, G40576019) and the Major Science and Technology International Corporation Program. (2002CB714001). Comments from two referees are highly appreciated.

References

Chang, C.P., Erickson, J.E., Liu, K.M., 1979. Northeasterly cold surges and near-equatorial disturbances over the Winter MONEX area during December 1974. Part I: Synoptic aspects. Mon. Weather Rev., vol. 107, pp. 812–829.

Chang, C.P., Zhang, Y.S., Li, T., 2000. Interannual and interdecadal variations of the east Asian monsoon and tropical pacific SSTs. Part II: meridional structure of the monsoon. J. Climate 13, 4326–4338.

Chang, C.P., Liu, C.H., Kuo, H.C., 2003. Typhoon Vamei: an equatorial tropical cyclone formation. Geophys. Res. Lett. 20, 501–504.

Chen, T.K., 1981. Study of the relationship between the South China Sea typhoon and the ocean temperature. Proceedings of the 1978 Typhoon Conference. Shanghai Science and Technology Press, Shanghai, pp. 256–259 (in Chinese).

Chen, L.S., Ding, Y.H., 1979. An Introduction to the Western Pacific Typhoon. China Science Press, Beijing, pp. 91–157 (in Chinese).

Chu, P.S., 2004. In: Murnane, R.J., Liu, K.-B. (Eds.), ENSO and Tropical Cyclone Activity. Hurricanes and Typhoons: Past, Present, and Potential. Columbia University Press, pp. 297–332.

Ding, Y.H., 1994. Monsoons over China, vol. 128–141. Kluwer Academic Publishers, Dordrecht. 419 pp.

Ding, Y.H., Li, C.Y., Liu, Y.J., 2004. Overview of the South China Sea Monsoon Experiment. Adv. Atmos. Sci. 21, 343–360.

Emanuel, K., 2003. Tropical cyclones. Annu. Rev. Earth Planet. Sci. 31, 75–104. doi:10.1146/annurev.earth.31.1000901.141259.

Fink, H.A., Speth, P., 1998. Tropical cyclones. Naturwissenschaften 85, 482–493.

Goldenberg, S.B., Landsea, C.W., Mestas-Nuñez, A.M., Gray, W.M., 2001. The recent increase in Atlantic hurricane activity: causes and implications. Science 293, 474–479.

Gray, W.M., 1968. Global view of the origin of tropical disturbances and storms. Mon. Weather Rev. 96, 669–700.

Harr, P.A., Chan, J., 2005. Monsoon impacts on tropical variability. In: Chang, C.P., Wang, B., Lau, N.C.G. (Eds.), The Global Monsoon System: Research and Forecast. WMO, Geneva Switzerland, pp. 512–542.

Johnson, R.H., Zimmerman, J.R., 1986. Modification of the boundary layer over the south China sea during a winter MONEX cold surge event. Mon. Weather Rev. 114, 2004–2115.

Liang, B.Q., 1991. The Tropical Atmospheric Circulation System over the South China Sea. China Meteorology Press, Beijing. (in Chinese).

Liang, J.P., 1998. Cloud imagine analysis of weather systems in the Nansha Islands and adjacent areas. In: Zhang, Q.R., Liang, B.Q. (Eds.), The Studies on the Interaction of the Air–Sea and the Property of Synoptic Climatology in the Nansha Islands Waters. Science Press, Beijing, pp. 173–182 (in Chinese).

Liang, B.Q., Wang, T.M., Zhou, X.M., 1998. The statistical analysis of the tropical cyclone in the Nansha Islands waters. In: Zhang, Q.R., Liang, B.Q. (Eds.), The Studies on the Interaction of the Air–Sea and the Property of Synoptic Climatology in the Nansha Islands Waters. Science Press, Beijing, pp. 163–172 (in Chinese).

Lighthill, J., 1998. Fluid mechanics of tropical cyclones. Theoret. Comput. Fluid Dynamics 10, 3–21.

Liu, Q.Y., Xia, J., Xie, S.P., Liu, W.T., 2004. A gap in the Indo-Pacific warm pool over the South China Sea in boreal winter: seasonal development and interannual variability. J. Geophys. Res. 109, C07012. doi:10.1029/2003JC002179.

Neumann, C., 1993. Global overview. In: Holland, G.J. (Ed.), Global Guide to Tropical Cyclone Forecasting, WMO/TD-560. World Meteorological Organization, Geneva, pp. 3.1–3.46.

Rayner, N.A., Parker, D.E., Horton, E.B., Folland, C.K., Alexander, L.V., Rowell, D.P., Kent, E.C., Kaplan, A., 2003. Global analyses of sea surface temperature, sea ice, and night marine air temperature since the late nineteenth century. J. Geophys. Res. 108, D4407. doi:10.1029/2002JD002670.

Su, J., 2004. Overview of the South China Sea circulation and its influence on the coastal physical oceanography outside the Pearl River Estuary. Cont. Shelf Res. 24, 1745–1760.

Tao, S., Chen, L., 1987. A review of recent research on East Asian summer monsoon in China. Monsoon Meteorology. Oxford University Press, pp. 60–92.

Wang, B., Fan, Z., 1999. Choice of south Asian summer monsoon indices. Bull. Am. Meteorol. Soc. 80, 629–638.

Wang, Z.X., He, S.X., 1979. A tropical cyclones developed from a South China Sea front depression. In: Institute, of Atmosphere Physics (Ed.), Typhoon and Tropical Circulation, vol. 8. Science Press, pp. 52–65.

Wang, B., Wu, R.G., 1997. Peculiar temporal structure of the South China Sea summer monsoon. Adv. Atmos. Sci. 14, 177–194.

Wang, G.H., Chen, D., Su, J., submitted for publication. A mechanism of eddy genesis in the eastern South China Sea. Geophys. Res. Lett.

Xie, S.P., Xie, Q., Wang, D.X., Liu, W.T., 2003. Summer upwelling in the South China Sea and its role in regional climate variations. J. Geophys. Res. 108 (C8), 3261. doi:10.1029/2003JC001876.

Xie, S.-P., Xu, H., Saji, N.H., Wang, Y., Liu, W.T., 2006. Role of narrow mountains in large-scale organization of Asian monsoon convection. J. Climate 19, 3420–3429.

Zhang, Y., Sperber, K.R., James, S.B., 1997. Climatology and interannual variation of the East Asian winter monsoon: results from the 1979–95 NCEP/NCAR reanalysis. Mon. Weather Rev. 125, 2605–2619.